ADVANCES IN CHEMISTRY SERIES 226

Electron Transfer in Biology and the Solid State

Inorganic Compounds with Unusual Properties

Michael K. Johnson, EDITOR
R. Bruce King, EDITOR
Donald M. Kurtz, Jr., EDITOR
Charles Kutal, EDITOR
Michael L. Norton, EDITOR
Robert A. Scott, EDITOR

University of Georgia

Developed from a symposium sponsored
by the Division of Inorganic Chemistry
at the Biennial Inorganic Chemistry Symposium
of the American Chemical Society,
Athens, Georgia,
March 1–4, 1989

American Chemical Society, Washington, DC 1990

CONTENTS

23

Stabilization of Conducting Heteroaromatic Polymers in Large-Pore Zeolite Channels

Thomas Bein[1], Patricia Enzel[1], Francois Beuneu[2], and Libero Zuppiroli[2]

[1]Department of Chemistry, University of New Mexico, Albuquerque, NM 87131
[2]Laboratoire des Solides Irradiés, S. E. S. I., École Polytechnique, F-91128 Palaiseau Cedex, France

Different strategies to encapsulate polymeric chains in ordered hosts are discussed. Pyrrole was polymerized as a model within the crystalline channel system of faujasite (three-dimensional) and mordenite (one-dimensional) zeolite molecular sieves. Polymerization required the presence of an intrazeolite oxidant such as ferric or cupric ions. No reaction was observed with the Na and Fe(II) forms of the zeolites. The yield of the reaction was highest with vapor-phase pyrrole, and it was low in aqueous solvents. The systems were characterized with a combination of electronic, infrared, and Raman spectroscopic data. Electron spin resonance measurements were used to explore the transport properties, and preliminary bulk powder conductivity measurements were performed to evaluate potential conduction paths on the outside of the zeolite crystals. The intrazeolite heteroaromatic polymer chains represent the first example of host-stabilized one-dimensional molecular conductors, or molecular wires.

THE DISCOVERY OF DOPED CONJUGATED POLYMERS has generated substantial research interest, both at the fundamental level and in view of possible applications (*1–3*). These polymers include doped polyacetylene, polyaniline, polypyrrole, and other polyheterocycles. Potential applications based on the conducting properties of these systems range from light-weight batteries, antistatic equipment, and microelectronics to speculative concepts such as "molecular electronic" devices (*4*, *5*).

0065–2393/90/0226–0433$06.00/0

Polypyrrole (PPy), for example, has been extensively studied in the form of thin films deposited on electrode surfaces (*6*). Electrochemical oxidative polymerization of pyrrole with anions (e.g., ClO_4^-, HSO_4^-) present in solution results in relatively air-stable, highly conducting films. Polypyrrole can also be prepared via chemical oxidation of pyrrole with Cu(II) or Fe(III) salts in solution (*7–10*). The proposed reaction path (*6*) via cation radicals is shown in Scheme I.

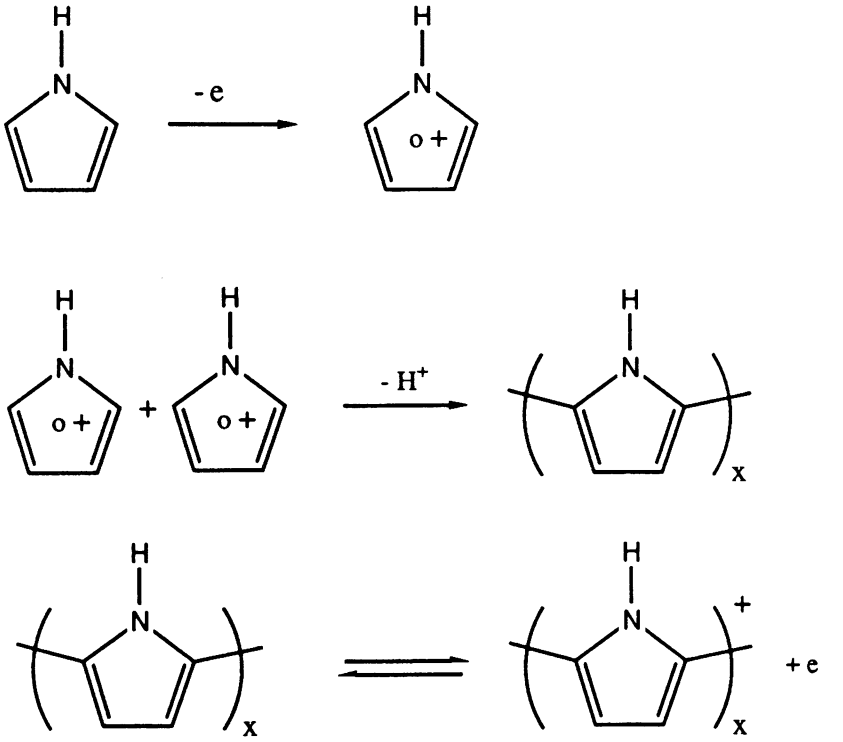

Scheme I. Oxidative polymerization of pyrrole.

In contrast to inorganic semiconductors that are characterized by three-dimensional covalent bonding and high carrier mobilities and are adequately described by rigid-band models, interactions in organic polymers are highly anisotropic (*11*). Atoms are covalently linked along the chains, whereas interchain interactions are much weaker; these structural features can cause collective instabilities such as Peierls distortions. Doping occurs by charge transfer between the intercalated dopant molecules or atoms and the organic chains, and it can result in substantial local relaxations of the chain geometry. New localized electronic states in the gap are introduced by these charge-transfer-induced local geometric modifications of the polymer.

In heteroaromatic polymers such as PPy, the ground state is nonde-

generate; the ground-state geometry with aromatic structure within rings and single bonds between rings is more stable than the corresponding quinoid resonance structure. Because the quinoid structure has a smaller band gap (lower ionization potential and larger electron affinity), the introduction of a charge on the chain can result in relaxation from the aromatic to the quinoid structure. The resulting electronic structure of PPy as a function of doping is depicted schematically in Figure 1.

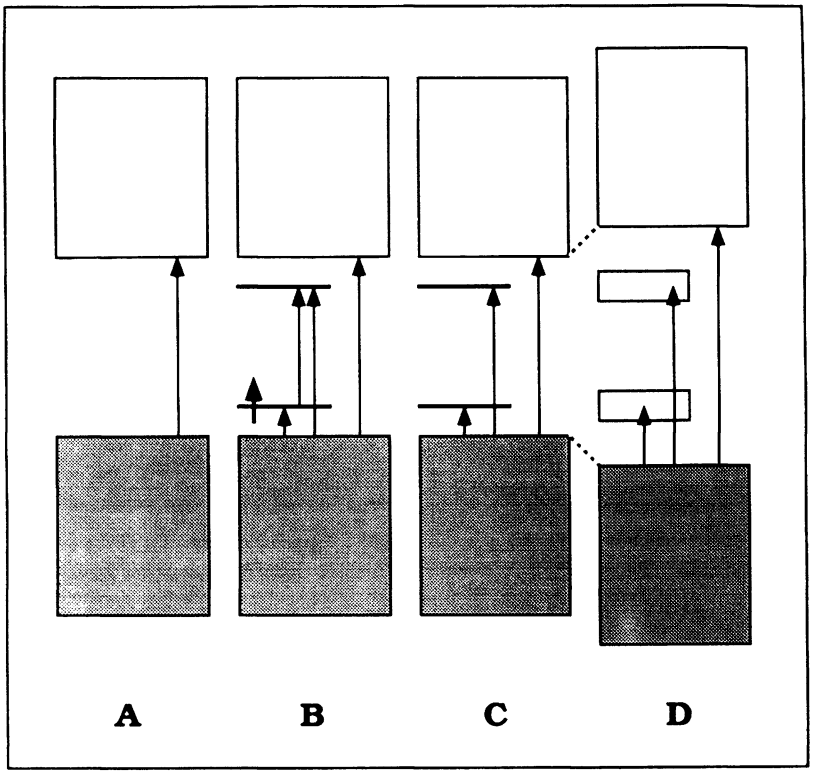

Figure 1. Band structure of polypyrrole as a function of doping level (schematic). Key: A, neutral polymer; B, polaron (+), spin = ½, three new transitions; C, bipolaron (++), spin = 0, two transitions; D, heavily doped, bipolaron bands.

Recent studies (*12*, *13*) conclude that at low doping levels, the chains are ionized to produce a radical cation (polaron) that is "pinned" to the counterion and does not contribute significantly to the conductivity. At higher doping levels, polarons can combine or ionize to form spinless dications (bipolarons) that are associated with a quinoid segment extending over four to five rings. The bipolarons are assumed to transfer charge via interchain hopping that corresponds to the observed spinless conductivity.

This model is consistent with the absence of Pauli susceptibility in the highly conducting form of PPy (*13*).

The study of the conduction mechanism of these polymers has been impeded by the low level of structural definition of most samples. The amorphous products of electrochemical and chemical oxidative polymerization reactions present a wide range of possible interchain interactions (e.g., islands with microcrystalline order separated by amorphous regions, unknown degrees of cross-linking, or bundles of fibers combined in disordered arrays).

Fundamental studies of the electronic structure and conduction mechanism of conducting polymers would benefit substantially if the low-dimensional structures were available as isolated, structurally well-defined, chemically accessible entities. The goal of our research program in this area is to design corresponding model systems via encapsulation of polymeric chain conductors in low-dimensional, crystalline host lattices, particularly in zeolites. Embedding a single chain in a zeolite matrix is also of interest, because the electronic properties of single chains in the solid state are not easily available. Chain segments, even if short, are interesting because of potential quantum-size effects on the electronic structure that have been observed in colloidal semiconductor systems, both in suspension and stabilized in zeolite host systems (*14–17*).

This chapter reports on our initial progress (*18*) in the encapsulation of heteroaromatic conjugated polymers in large-pore zeolites, particularly polypyrrole. We recently succeeded in synthesizing polyaniline (*19, 20*) and polythiophene (*21*) in zeolite Y and mordenite. Previously reported strategies for the design of low-dimensional structures are discussed in the following sections.

Stabilization of Low-Dimensional Polymer Structures

Urea and other organic hosts have been explored for the radiation-induced inclusion polymerization of clathrated monomers such as butadiene (*22*). Well-studied examples include vinyl chloride, acrylonitrile and butadiene in urea, butadiene, pentadiene in deoxycholic acid, and ethylene and propylene in perhydrotriphenylene. Polymerization in the clathrates is usually induced by exposure to high-energy radiation that produces radicals derived from host and guest molecules, and proceeds via a living radical mechanism. Inclusion polymerization can result in a high degree of steric control of the resulting included polymer chains. To our knowledge, no conjugated, conducting clathrate systems have yet been synthesized.

If the dimension of channel-shaped hosts is extended such that unhindered diffusion of monomers can occur, conducting polymers can be formed on an electrode surface. Polypyrrole and poly(3-methylthiophene) fibrils with diameters between 0.03 and 1 μm at 10-μm length have been synthesized

in microfilter membranes (Nuclepore) (*23*, *24*). Stretch alignment has often been employed to create directional anisotropy in preformed polymers, such as in polyacetylene (*25–27*). Liquid crystal polymerization under a magnetic field is an alternative technique to achieve alignment (*28*, *29*).

Inorganic layer compounds have been explored for the polymerization of organic compounds in two dimensions (*30*). Prominent examples are based on layer perovskite halide salts with the general formula $(RCH_2NH_3)_2MX_4$, where M is a divalent metal such as Mn, Fe, Cu, and Cd, and X is a halide ion (*31*). The organic cations separate the layers formed by the metal halides. If the organic cations contain 2,4-diene units, the corresponding layered compounds can be polymerized with gamma irradiation to form 1,4-disubstituted *trans*-polybutadienes (*32*, *33*). However, if related diacetylene-containing layer perovskites are polymerized, the original lattice is gradually broken up (*30*). Recent studies explored the intercalative polymerization of pyrrole, thiophene, and aniline in layered FeOCl (and V_2O_5) (*34–36*); this polymerization exploits the well-established oxidative intercalation of organic molecules (*37*, *38*) with concomitant reduction of FeOCl. It was found that pyrrole intercalated into FeOCl and polymerized to result in an inorganic-conducting polymer hybrid structure with an interlayer spacing increased by 5.23 Å.

Other two-dimensional systems that will not be discussed here include the electropolymerization of aniline intercalated in montmorillonite clay (*39*) and polymerizations in Langmuir–Blodgett films or bilayer membranes (*40*).

Efforts to form composites between polypyrrole and a variety of porous materials such as paper, cloth, or wood have been based on an approach comparable to that used in the present study. Typically, the respective material was impregnated with an oxidant such as $FeCl_3$ (*41*, *42*) and subsequently contacted with pyrrole vapor or solution. Polypyrrole (and polyaniline) have been included in perfluorosulfonated ionomer membranes (Nafion) by stepwise treatment with aqueous ferric chloride and the monomers (*43*).

This brief survey indicates that no single chains of conjugated systems with long-range order have yet been stabilized in solid matrices. We will show that our approach, based upon intrazeolite polymerization reactions, succeeds in the formation of such systems.

Zeolites as Microporous Host Structures

Zeolites (*44–47*) are crystalline open framework metal oxide structures (classically aluminosilicates with hydrophilic surfaces) with pore sizes between 3 and 12 Å and exchangeable cations compensating for the negative charge of the framework. The topologies of these systems include one-dimensional channels, intersecting two-dimensional channels, and three-dimensional open frameworks. Recent developments include hydrophobic structures

with compositions close to SiO_2 (*48*), incorporation of transition metals into the framework (*49*), and the discovery of metal aluminophosphate sieves (*50*). Alkali metal cations, possibly coordinated to oxygen–metal rings with C_{3v} or C_{2v} symmetry in zeolite Y (Figure 2), can be exchanged for transition metal ions and the system can be heat-treated to induce cation migration and removal of water. Table I presents a brief description of zeolite structure types used in this study.

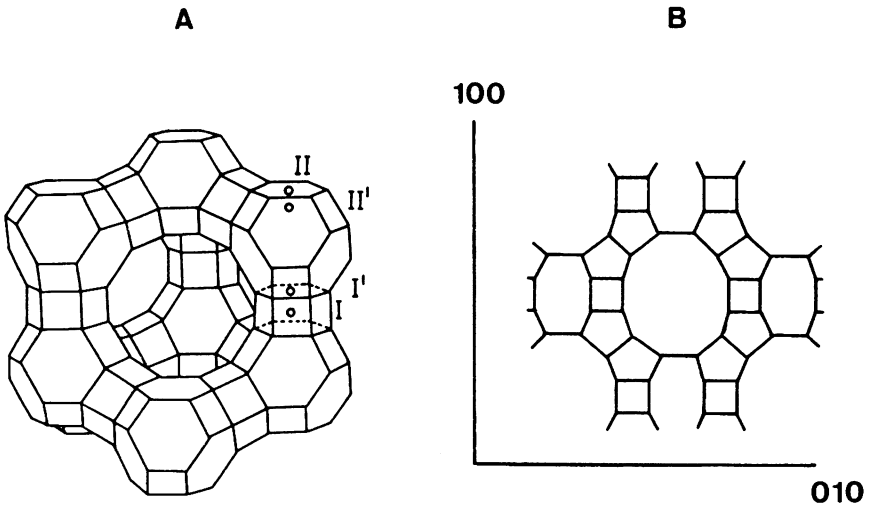

Figure 2. Structure of faujasite (A) and mordenite (B).

These features make zeolites extremely attractive candidates as hosts for polymeric conductors. They offer well-defined, stable crystalline channel structures with dimensions at the molecular level. The nature of the internal surface, as determined by cation type and other factors, will affect the dipolar and redox surface interactions and diffusion rates of polar versus nonpolar monomers. Previous work related to the present study includes the catalytic formation of polyacetylene from acetylene on the external surface of CoY and NiY zeolites (*51*) and on KX zeolite (*52*).

This chapter presents recent results on the successful encapsulation of polypyrrole chains in large-pore three-dimensional and one-dimensional zeolite hosts. The host structures examined in this study include zeolite Y (three-dimensional channel system, 7.5-Å pores), mordenite (one-dimensional channels, 7-Å pores), and zeolite A (three-dimensional channels, 4.1-Å pores). Polypyrrole was oxidatively polymerized in Cu(II)- or Fe(III)-containing zeolite pores, such as

$$\text{NaY} + \text{FeSO}_4(\text{aq}) \xrightarrow{\text{N}_2} \text{NaFe(II)Y} \xrightarrow{\text{O}_2/350\ ^\circ\text{C}} \text{NaFe(III)Y} \xrightarrow[\text{(vapor/solvent)}]{\text{pyrrole}} \text{PPy/NaFe(II)Y} \quad (1)$$

Table I. Representative Zeolite Structure Types

Name	*Unit Cell, Composition*	*Cage Type*	*Main Channels, Å*[a]
LTA, Linde A	$[Na_{12}[(AlO_2)_{12}(SiO_2)_{12}]\ 27\ H_2O]_8$	α, β	4.1 ***
FAU, Faujasite	$Na_{58}[(AlO_2)_{58}(SiO_2)_{134}]\ 240\ H_2O$	β, 26-hedron(II)	7.4 ***
MOR, Mordenite	$Na_8[(AlO_2)_8(SiO_2)_{40}]\ 24\ H_2O$	complex 5-1	6.7 x 7.0 * ↔ 2.9 x 5.7 *

[a]The number of stars (*) at the channel description indicates the dimensionality of channel connections.

The intrazeolite oxidation of Fe(II) with oxygen probably involves the formation of Fe(III)–O–Fe(III) bridges in appropriate coordination sites (*53*), although generation of some amorphous iron oxide cannot be excluded (*54*).

The systems were characterized with a combination of electronic, infrared, and Raman spectroscopic data. Electron spin resonance (ESR) and conductivity measurements were used to explore the transport properties.

Experimental Details

Sample Preparation. ***Zeolite Precursor Materials.*** Fe(II)Y zeolite was prepared from the sodium form of zeolite Y (Linde LZ-Y52, Alfa) by conventional aqueous ion exchange with ferrous sulfate under nitrogen atmosphere and dried at 295 K under nitrogen (*54*). The resulting ferrous Y zeolite [unit cell compositions, based upon ion exchange, $Fe_6Na_{44}(AlO_2)_{56}(SiO_2)_{136}$ for solution loadings and $Fe_{10}Na_{36}(AlO_2)_{56}(SiO_2)_{136}$ for vapor-phase loadings] was heated under a flow of oxygen (40 mL/min) in a quartz tube reactor at a rate of 1 K/min to 370 K (10 h), then to 620 K (3 h), and subsequently evacuated for 2 h at that temperature to give Fe(III)Y. The color of the zeolite changed from white to light brown during this treatment. Ferrous mordenite (Fe(II)M) was similarly prepared from Na mordenite (LZM-5, Union Carbide) by ion exchange to give white $Fe_3Na_2(AlO_2)_8(SiO_2)_{40}$. This material was oxidized in a scheme similar to that used with ferrous Y and generated light brown Fe(III)M. Cu(II) forms of these zeolites and zeolite A were obtained by ion exchange with $Cu(NO_3)_2$, resulting in samples CuY, CuM, and CuA with 15, 2.5, and 8 Cu ions per unit cell (u.c.), respectively. Dehydrated sodium zeolites (heated at 1 K/min up to 720 K under vacuum, kept at 720 K for 10 h) and the metal-containing dry samples were stored under nitrogen in a glove box prior to use.

Bulk Polypyrrole. Bulk polypyrrole was prepared by chemical oxidation of pyrrole (Aldrich) with $FeCl_3 \cdot 6H_2O$ (Aldrich) according to published procedures (*7*, *8*, *55*). Oxidation with an oxidant:pyrrole ratio of 2.4 in aqueous solution at 292 K, carried out under nitrogen, represents the optimal reaction conditions for highest yield and conductivity (*7*).

Intrazeolite Polymerization of Pyrrole. Pyrrole was diffused into the pore system of the dry zeolites in a variety of solvents and via gas-phase adsorption (Table II). In the solvent reactions, 0.500 g of Fe(III)Y was suspended in a solution of 5.16 mg of pyrrole (0.077 mmol) in 50 mL of the respective solvent and stirred at 295 K for 15 h under nitrogen. Similarly, 0.500 g of Fe(III)M was reacted with 12.5 mg (0.187 mmol) of pyrrole. For the vapor-phase reactions, ~0.5 g of dry zeolite was weighed into a small quartz reactor, evacuated at a vacuum line at 1.33 mPa (10^{-5} torr), and equilibrated with 270 Pa (2 torr) of degassed pyrrole at 295 K for 1 h.

Characterization. Fourier transform infrared (FTIR) spectra were taken at 4-cm^{-1} resolution (Mattson Polaris instrument) and were analyzed with the ICON software. Electronic absorption spectra of the samples dispersed in glycerin were obtained with a spectrophotometer (PE 356) at 2-nm resolution. ESR spectra between 40 and 300 K were obtained with a Varian E-109 instrument operating at X-band frequencies. Conductivity measurements at 295 K were carried out with pressed wafers of the bulk polymers and of the zeolite powders by using the four-point technique (*56*). Resonance Raman spectra were generated by irradiating the sample with 5 mW at 457.9 nm. Scanning electron micrographs were taken with an Hitachi S-800 microscope.

Table II. Zeolite–Pyrrole Samples

Sample[a]	*Loading with Pyrrole*[b]	*Surface Capacity*[c]	*Reaction Time, h*	*Color*
NaY–V	41	0.2	1	white
NaM–V	2	0.06	1	white
Fe(II)Y–V	40	0.2	1	white
Fe(II)M–V	2	0.06	1	white
Fe(III)Y–V	39	0.2	1	black/turquoise
Fe(III)Y–W	2	0.2	15	light green
Fe(III)Y–T	2	0.2	15	grey/turquoise
Cu(II)Y–V	50	0.2	1	black/turquoise
Fe(III)M–V	1.0	0.06	1	turquoise
Fe(III)M–W	1.2	0.06	15	light green
Fe(III)M–T	1.2	0.06	15	light green
Cu(II)M–V	0.7	0.06	1	turquoise
Cu(II)A–V	0.3	0.3	1	very light green

[a]Abbreviations: Y, zeolite Y; M, mordenite; A, zeolite A; V, vapor phase; W, water; T, toluene.
[b]Molecules per unit cell.
[c]The surface capacities for 1-μm crystals are based on 0.6-nm diameter for pyrrole; normalized per zeolite unit cell.

Results and Discussion

If pyrrole is allowed to diffuse into large-pore zeolites that contain ferric ions, the color of the resulting adduct changes slowly from light brown to different shades of turquoise green and black. This striking reaction appears to be completed within a few minutes if the pyrrole is admitted as vapor into the dry zeolite, and within a few hours if diffused from solution (Table II). In contrast, pyrrole in zeolites containing only sodium ions or Fe(II) ions does not react to form colored products. Irrespective of pyrrole concentration and medium (different solvents or vapor phase), none of these blank experiments resulted in a color change of the sample (Table II). This behavior strongly suggests that pyrrole polymerizes to polypyrrole in a redox reaction that involves the intrazeolite ferric or cupric ions. Bulk polypyrrole has been synthesized chemically via oxidative coupling of pyrrole in various solutions and suspensions of ferric chloride. An overall reaction scheme in H_2O/C_2H_5OH solution has been proposed (57).

$$4C_4H_5N + 9FeCl_3 \cdot nH_2O \rightarrow (C_4H_3N)_4^+Cl^- + 8HCl + 9FeCl_2 \cdot nH_2O \quad (2)$$

The following discussion of the sample characteristics confirms the formation of intrazeolite polypyrrole.

Sample Characteristics. ***IR Spectra.*** Bulk polypyrrole is characterized by a broad IR absorption that extends from an electronic absorption band at ~1 eV (8000 cm^{-1}) down to about 1700 cm^{-1} and obscures the C–H and N–H vibrations of the polymer (6). The oxidized and the neutral forms

of the polypyrrole have very similar C–C and C–H pyrrole ring vibrations in the 1600–800-cm^{-1} region (*58*, *59*). In contrast to pyrrole, the ring vibrations of the polymer are relatively broad and can be distinguished from remaining unreacted monomer. The intrazeolite polypyrrole shows IR bands quite similar to the typical set of bands characteristic for bulk polypyrrole. However, certain shifts that vary with host and preparation conditions are observed (Figure 3). According to the electrical potential of the zeolite, the polymer chains should not exactly duplicate the bulk spectrum. For instance, bands of sample Fe(III)Y–V prepared from vapor phase occur at 1572 (1540), 1473 (1452), 1309 (1280–1300), and 790 (791) cm^{-1}. Positions of bulk polypyrrole are given in parentheses (*58*, *59*).

The IR spectra of zeolite Y samples show a higher concentration of polypyrrole than the mordenite samples, probably because of the higher pore volume fraction available in the former host. Intrazeolite PPy recovered after dissolution of the host in HF shows features very similar to those of the bulk polymer (Figure 3).

Formation of polypyrrole according to the oxidative reaction mechanism is expected to produce two protons per monomer. These protons must be accommodated in the zeolite, but the IR data of these samples do not show clear hydroxyl features. This result is not surprising in view of the strong electronic absorption extending beyond the high-energy part of the spectrum. Similar observations are noted in the polypyrrole–FeOCl system (*60*). With its pronounced acid–base and ion-exchange properties, the zeolite framework (or intrazeolite Fe species) is expected to accommodate the additional proton concentration.

Raman Spectra of Intrazeolite Polypyrrole. Bulk polypyrrole is known to exhibit weak Raman spectra, but resolved bands in the 800–1600 cm^{-1} range have recently been obtained with smooth films formed on electrode surfaces (*61*). Resonance Raman spectra of polypyrrole–zeolite samples (e.g., sample Fe(III)Y–V) show weak but resolved bands at 1598 and 1418 cm^{-1} that correspond to the vibrations at 1591 and 1418 cm^{-1} reported for polypyrrole film grown on a Pt electrode (*62*).

Location of the Polymer Chains. It is clear from the combined spectroscopic evidence discussed and from the electronic spectra that polypyrrole forms when pyrrole reacts with zeolites containing ferric and cupric ions. In the context of synthetic strategies for the design of molecular "wires", it is important to determine the location of the polypyrrole with respect to the host. A film of polypyrrole at the outside of the zeolite crystals would not constitute a system of isolated molecular chains. Because of the insoluble nature of the polymer, extraction experiments do not provide much information. However, significant indirect evidence confirms the picture of zeolite-encapsulated polypyrrole.

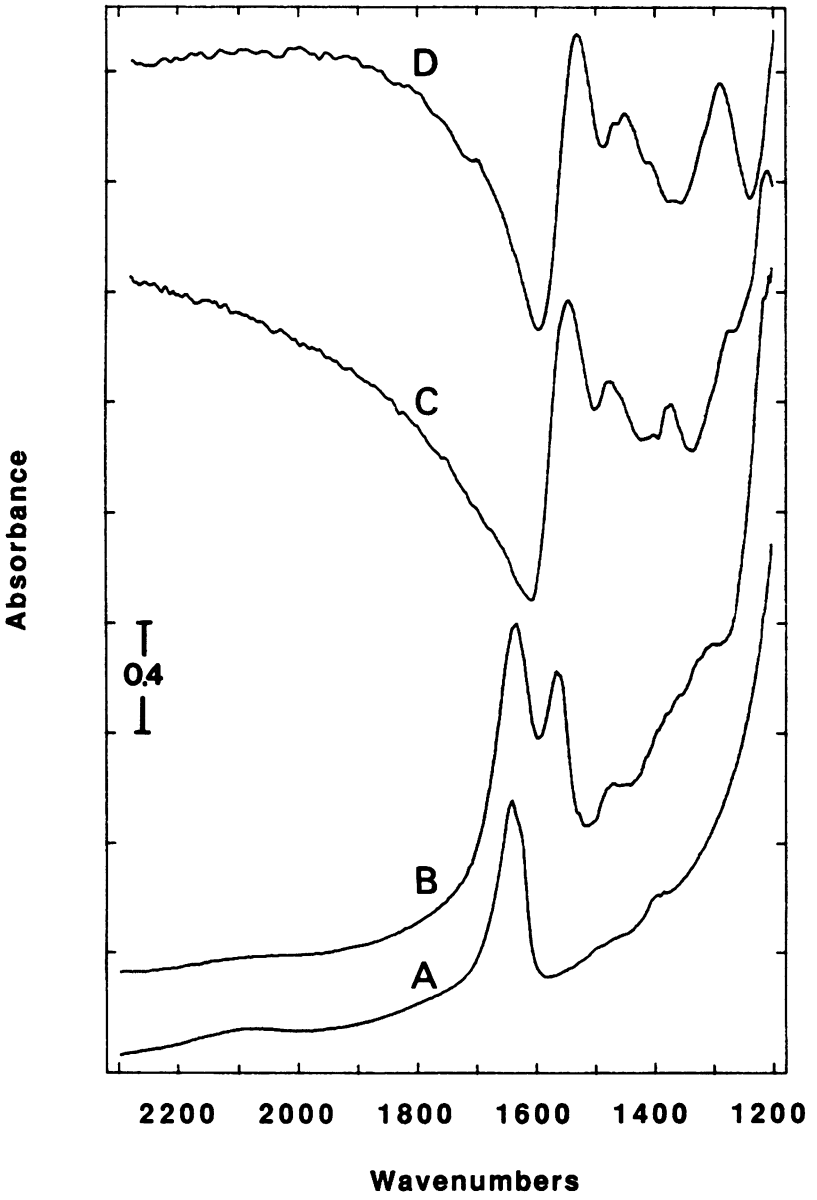

Figure 3. IR spectra (KBr pellets) of samples. Key: A, NaY; B, Fe(III)–V; C, PPy extracted from Fe(III)–V; and D, bulk polypyrrole.

The polypyrrole is not formed in either the Na or Fe(II) forms of the zeolites. Therefore the polymerization is dependent upon a redox reaction with the predominantly intrazeolite Fe(III) and Cu(II) ions. The polymerization reaction is one to two orders of magnitude slower in the zeolite host than it is in homogeneous solution. This retardation indicates diffusional limitations for the pyrrole migrating into the channel system. Finally, an analysis of the uptake of monomer into the zeolite confirms the same conclusions. Table II lists the uptake of monomer in different zeolite hosts and compares the values with those expected from monolayer-coating on the surface of crystals with 1.0-μm diameter.

These results show that far more monomer can be accommodated within the zeolite pores than expected for surface adsorption (the values for mordenite are smaller because of a smaller unit cell). Furthermore, we find that pyrrole is not adsorbed into the pore system of zeolite A, as expected from its smaller pore diameter (4.1 Å), but the uptake corresponds very well with the value expected for surface adsorption. Thus, if the monomer is excluded from the interior of the zeolite, not more than about one monolayer is adsorbed at the crystal surface.

On the basis of the stoichiometry of monomer loading versus Fe(III) or Cu(II) present in the zeolite, it can be concluded that in the zeolite Y samples prepared via vapor-phase saturation, only about 20% of the adsorbed pyrrole molecules can be oxidatively coupled. The remainder of the monomer is probably still present in the zeolite pores. The maximum exchange level of ~10 Fe/u.c. was chosen to avoid potential zeolite lattice breakdown (*54*). In all other samples, the relative excess of Fe(III) is expected to suffice for a complete reaction.

The rate of polymerization as estimated from the rate of sample coloration is much faster in a three-dimensional zeolite (zeolite Y) than in a one-dimensional pore system (mordenite). All these data taken together provide clear evidence that the polymerization of pyrrole proceeds within the zeolite channel system if the monomer has access into the pores.

The reaction medium has an interesting influence on the intrazeolite concentration of the polymer. In contrast to homogeneous solution preparations, water is one of the most unfavorable media for intrazeolite polymerizations. Reactions in hydrocarbon solvents and via vapor-phase loading result in the highest polymer yields. Possibly, water screens the intrazeolite redox-active metal ions from the monomer molecules.

Electronic Structure and Transport Properties. ***Electronic Spectra.*** The Fe(III)-containing zeolite hosts exhibit a broad absorption between 300 and 450 nm, which accounts for the light brown color of these zeolites. The electronic spectra of the sodium and ferrous forms do not differ significantly. If pyrrole is adsorbed into the sodium forms and ferrous forms of both zeolites, the optical spectra in the visible range remain unchanged.

In contrast, the spectrum of sample Fe(III)Y–V shows two important new features at 400–500 nm (~2.7 eV) and at energies lower than 650 nm (Figure 4D).

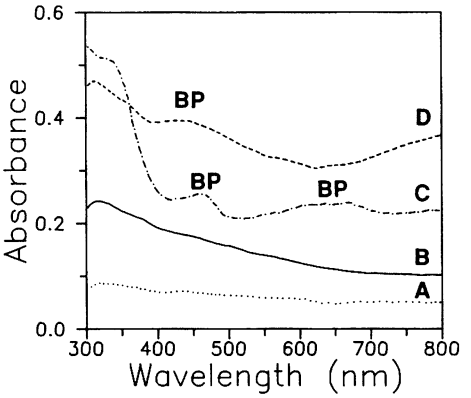

Figure 4. Electronic absorption spectra of samples. Key: A, NaM; B, NaY; C, Fe(III)M–V; and D, Fe(III)Y–V.

The spectral features of the samples prepared in toluene and with vapor-phase pyrrole are more pronounced than those of the other samples. The red absorption of Y zeolite samples is generally stronger than that of mordenite. In addition, the vapor-phase product Fe(III)M–V shows a feature between 520 and 700 nm (~2.0 eV, Figure 4C). Absorption maxima at 2.3 and 0.7 eV have been observed with electrochemically formed, highly doped polypyrrole; the higher energy band shifted to lower values at lower oxidation levels (*63*). On the basis of the electronic model discussed, we assign the bands at 2.7 and 2.0 eV and that in the near-IR region to bipolaron absorptions that are typical of polypyrrole at different oxidation levels. Thus, we can conclude that the oxidation level of PPy in faujasite is high and that there is probably a bimodal distribution of highly oxidized and medium oxidation levels of polypyrrole in mordenite. The conduction band absorption appears to occur in the near-UV range. Finally, the spectrum of Cu(II)A–V does not exhibit any of the features observed with the large-pore samples (not shown).

ESR Spectra. Polypyrrole in Fe(III)Y–V and Fe(III)M–V shows an ESR signal at proportionality factor $g = 2.0027$, very similar to the bulk value (*13*). The spin densities calculated from the ESR lines and the monomer loadings are 3×10^{-4} per pyrrole monomer in sample Fe(III)Y–V, and 9×10^{-4} per pyrrole monomer in sample Fe(III)M–V. Because the degree of polymerization is not precisely known, these numbers are lower limits with respect to the polymer content. The corresponding spin susceptibilities show Curie behavior between ~40 and 300 K (Figure 5A). These data are explained

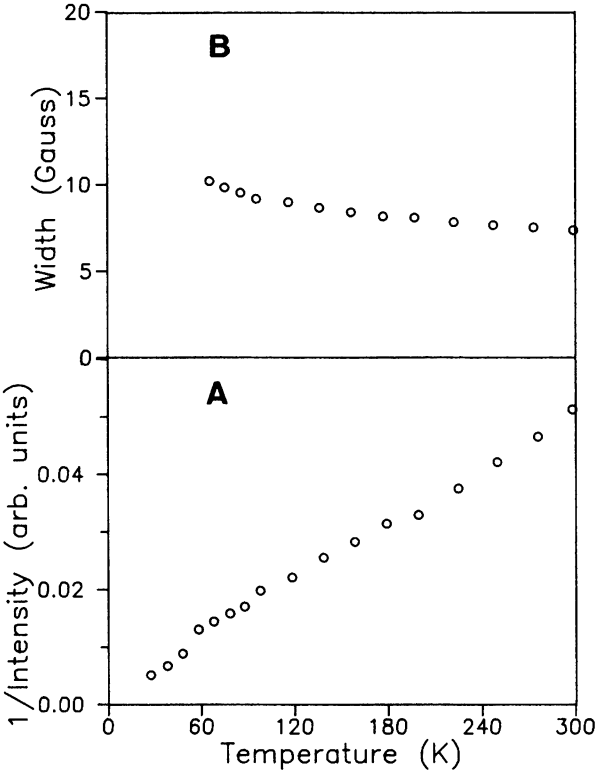

Figure 5. ESR data of sample Fe(III)Y–V. Key: A, Curie behavior; B, line width as function of temperature.

with a small concentration of paramagnetic defects that have also been observed in bulk polypyrrole samples, probably a result of defects in the π system of the polymer chain (*13*). Surprisingly, the line width of the ESR resonance of intrazeolite polymers is at the order of 10 G (Figure 5B), in contrast to a typical value of 0.2 G for pure bulk polymers. In the bulk, the line width can be reversibly increased to similar values by adding several weight percents of oxygen (*13*). Because our samples were measured in vacuo, the most likely explanation for the large line width is an intrinsic dipolar interaction between the polymer chains and the charged zeolite channel walls.

Conductivity measurements of polypyrrole–zeolite samples show dramatic differences compared to bulk properties. Although values for bulk polypyrrole are at the order of 10 S/cm (*8*), the zeolite samples have powder conductivities below 10^{-9} S/cm. These dc measurements are not considered to give the conductivity of the polymer chains because shorter chains could reside in the zeolite cages without providing a continuous conduction path. This striking result is expected, however, because "perfect" samples that

have clean, uncoated dielectric crystal surfaces could not provide any continuous conducting path through a pressed wafer. Thus, this observation provides additional evidence for the strictly intrazeolite location of the conjugated polymers. Initial X-ray photoelectron spectroscopy measurements of related intrazeolite polyaniline samples clearly indicate a depletion of nitrogen at the zeolite crystal surfaces.

Conclusions

This study shows that pyrrole can be oxidatively polymerized in the channel system of zeolite molecular sieves. Comprehensive spectroscopic characterization identifies the nature of the polymerization product and provides strong evidence for encapsulation within the channel systems. This approach to isolated "molecular wires" via intrahost polymerization is presently being extended to a variety of other organic and inorganic conducting systems. More detailed studies will address issues such as the intrazeolite polymer chain length, effects of host pore size, and transport properties of the resulting low-dimensional systems.

Acknowledgments

Instrumentation used in this work was acquired with funding from the National Science Foundation. We thank A. Galuska (Sandia National Laboratories) for X-ray photoelectron spectroscopy experiments and B. Crawford (University of New Mexico) for Raman measurements.

References

1. *Proceedings of the International Conference on Science and Technology of Synthetic Metals;* Aldissi, M., Ed.; *Synth. Met.* **1989,** *28*(1–3) and *29*(1).
2. *Handbook of Conducting Polymers;* Skotheim, T. A., Ed.; Marcel Dekker: New York, 1986; Vol. 1.
3. *Conducting Polymers: Special Applications;* Alcacer, L., Ed.; D. Reidel: Dordrecht, Netherlands, 1987.
4. *Molecular Electronic Devices;* Carter, F. L., Ed.; Marcel Dekker: New York, 1982.
5. *Molecular Electronic Devices II;* Carter, F. L., Ed.; Marcel Dekker: New York, 1987.
6. Street, G. B. *Handbook of Conducting Polymers;* Skotheim, T. A., Ed.; Marcel Dekker: New York, 1986; Vol. 1, p 265.
7. Armes, S. P. *Synth. Met.* **1987,** *20,* 365.
8. Rapi, S.; Bocchi, V.; Gardini, G. P. *Synth. Met.* **1988,** *24,* 217.
9. Chao, T. H.; March, J. *J. Polym. Sci., Polym. Chem. Ed.* **1988,** *26,* 743.
10. Pron, A.; Suwalski, J.; Lefrant, S. *Synth. Met.* **1987,** *18,* 25.
11. Bredas, J. L.; Themans, B.; Andre, J. M.; Chance, R. R.; Silbey, R. *Synth. Met.* **1984,** *9,* 265.

12. Genoud, F.; Guglielmi, M.; Nechtschein, M.; Genies, E.; Salmon, M. *Phys. Rev. Lett.* **1985,** *55,* 118.
13. Scott, J. C.; Pfluger, P.; Krounbi, M. T.; Street, G. B. *Phys. Rev. B* **1983,** *28,* 2140.
14. Parise, J. B.; MacDougall, J.; Herron, N.; Farlee, R. D.; Sleight, A. W.; Wang, Y.; Bein, T.; Moller, K.; Moroney, L. *Inorg. Chem.* **1988,** *27,* 221.
15. Wang, Y.; Herron, N. *J. Phys. Chem.* **1987,** *91,* 257.
16. Herron, N.; Wang, Y.; Eddy, M. M.; Stucky, G. D.; Cox, D. E.; Moller, K.; Bein, T. *J. Am. Chem. Soc.* **1989,** *111,* 530.
17. Moller, K.; Eddy, M. M.; Stucky, G. D.; Herron, N.; Bein, T. *J. Am. Chem. Soc.* **1989,** *111,* 2564.
18. Bein, T.; Enzel, P. *Angew. Chem.* **1990,** in press.
19. Bein, T.; Enzel, P. *Synth. Met.* **1989,** *29,* E163.
20. Enzel, P.; Bein, T. *J. Phys. Chem.* **1989,** *93,* 6270.
21. Enzel, P.; Bein, T. *J. Chem. Soc., Chem. Commun.* **1989,** 1326.
22. Farina, M.; Di Silvestro, G.; Sozzani, P. *Crystallographically Ordered Polymers;* Sandman, D. J., Ed.; ACS Symposium Series 337; American Chemical Society: Washington, DC, 1987; 79, and references cited therein.
23. Penner, R. M.; Martin, C. R. *J. Electrochem. Soc.* **1986,** *133,* 2206.
24. Cai, Z.; Martin, C. R. *J. Am. Chem. Soc.* **1989,** *111,* 4138.
25. Mizoguchi, K.; Kume, K.; Masubuchi, S.; Shirakawa, H. *Synth. Met.* **1987,** *17,* 405.
26. Horton, M. E.; Friend, R. H.; Foot, P. J. S.; Billingham, N.; Calvert, P. D. *Synth. Met.* **1987,** *17,* 395.
27. Mulazzi, E.; Brivio, G. P.; Lefrant, S.; Faulques, E.; Perrin, E. *Synth. Met.* **1987,** *17,* 325.
28. Akagi, K.; Katayama, S.; Shirakawa, H.; Araya, K.; Muko, A.; Narahara, T. *Synth. Met.* **1987,** *17,* 241.
29. Park, Y. W.; Lee, Y. S.; Kim, Y. K.; Lee, C. K.; Park, C.; Shirakawa, H.; Akagi, K.; Kitagaki, T.; Katayama, S. *Synth. Met.* **1987,** *17,* 539.
30. Day, P. *Handbook of Conducting Polymers;* Skotheim, T. A., Ed.; Marcel Dekker: New York, 1986, 117.
31. Arend, H.; Huber, W.; Mischgofsky, F. H.; Richter-van Leeuwen, G. K. *J. Cryst. Growth* **1978,** *43,* 213.
32. Tieke, B.; Chapuis, G. *Crystallographically Ordered Polymers;* Sandman, D. J., Ed.; ACS Symposium Series 337; American Chemical Society: Washington, DC, 1987; p 61.
33. Tieke, B.; Wegner, G. *Makromol. Chem. Rapid Commun.* **1981,** *2,* 543.
34. Kanatzidis, M. G.; Tonge, L. M.; Marks, T. J.; Marcy, H. O.; Kannewurf, C. R. *J. Am. Chem. Soc.* **1987,** *109,* 3797.
35. Kanatzidis, M. G.; Hubbard, M.; Tonge, L. M.; Marks, T. J.; Marcy, H. O.; Kannewurf, C. R. *Synth. Met.* **1989,** *28,* C89.
36. Kanatzidis, M. G.; Wu, C.-G.; Marcy, H. O.; Kannewurf, C. R. *J. Am. Chem. Soc.* **1989,** *111,* 4139.
37. Kauzlarich, S. M.; Stanton, J. L.; Faber, J., Jr.; Averill, B. A. *J. Am. Chem. Soc.* **1986,** *108,* 7946.
38. Kauzlarich, S. M.; Teo, B. K., Averill, B. A. *Inorg. Chem.* **1986,** *25,* 1209.
39. Inoue, H.; Yoneyama, H. *J. Electroanal. Chem. Interfacial Electrochem.* **1987,** *233,* 291.
40. Kuo, T.; O'Brien, D. F. *J. Am. Chem. Soc.* **1988,** *110,* 7571, and references cited therein.
41. Bocchi, V.; Gardini, G. P. *J. Chem. Soc., Chem. Commun.* **1986,** 148.
42. Bjorklund, R. B.; Lundstrom, I. *J. Electron. Mater.* **1984,** *13,* 211.

43. Aldebert, P.; Audebert, P.; Armand, M.; Bidan, G.; Pineri, M. *J. Chem. Soc., Chem. Commun.* **1986,** 1636.
44. Breck, D. W. *Zeolite Molecular Sieves;* R. E. Krieger: Malabar, FL, 1984.
45. *Zeolites: Facts, Figures, Future;* Jacobs, P. A.; van Santen, R. A., Eds.; *Stud. Surf. Sci. Catal.* **1989,** *49,* Elsevier: Amsterdam.
46. *New Developments in Zeolite Science and Technology;* Murakami, Y.; Iijima, A; Ward, J. W., Eds.; Kodansha: Tokyo, 1986.
47. Szostak, R. *Molecular Sieves: Principles of Synthesis and Identification;* Van Nostrand Reinhold: New York, 1989.
48. Kokotailo, G. T.; Lawton, S. L.; Olson, D. H.; Meier, W. M. *Nature* **1978,** *272,* 437.
49. Ball, W. J.; Dwyer, J.; Garforth, A. A.; Smith, W. J. *New Developments in Zeolite Science and Technology;* Murakami, Y.; Iijima, A.; Ward, J. W., Eds.; Kodansha: Tokyo, 1986; p 137.
50. Messina, C. A.; Lok, B. M.; Flanigen, E. M. U.S. Patent 4 544 143, 1985.
51. Dutta, P. K.; Puri, M. *J. Catal.* **1988,** *111,* 453.
52. Heaviside, J.; Hendra, P. J.; Tsai, P.; Cooney, R. P. *J. Chem. Soc., Faraday Trans. 1* **1978,** *74,* 2542.
53. Dalla Betta, R. A.; Garten, R. L.; Boudart, M. *J. Catal.* **1976,** *41,* 40.
54. Pearce, J. R.; Mortier, W. J.; Uytterhoeven, J. B.; Lunsford, J. H. *J. Chem. Soc., Faraday Trans. 1* **1981,** *77,* 937.
55. Myers, R. E. *J. Electron. Mater.* **1986,** *15,* 61.
56. Smits, F. M. *Bell Syst. Tech. J.* **1958,** *37,* 711.
57. Pron, A.; Kucharski, Z.; Budrowski, C.; Zagorska, M.; Krichene, S.; Suwalski, J.; Dehe, G.; Lefrant, S. *J. Chem. Phys.* **1985,** *83,* 5923.
58. Neoh, K. G.; Tan, T. C.; Kang, E. T. *Polymer* **1988,** *29,* 553.
59. Zagorska, M.; Pron, A.; Lefrant, S.; Kucharski, Z.; Suwalski, J.; Bernier, P. *Synth. Met.* **1987,** *18,* 43.
60. Kanatzidis, M. G., personal communication; see also refs. 34, 35.
61. Cheung, K. M.; Smith, B. J. E.; Batchelder, D. N.; Bloor, D. *Synth. Met.* **1987,** *21,* 249.
62. Olk, C. H.; Beetz, C. P., Jr.; Heremans, J. *J. Mater. Res.* **1988,** *3,* 984.
63. Kaufman, J. H.; Colaneri, N.; Scott, J. C.; Kanazawa, K. K.; Street, G. B. *Mol. Cryst. Liq. Cryst.* **1985,** *118,* 171.

RECEIVED for review May 1, 1989. ACCEPTED revised manuscript October 17, 1989.